JOURNAL OF GEOPHYSICAL RESEARCH, VOL. 99, NO. D11, PAGES 23,071–23,078, NOVEMBER 20, 1994

Daily surface wind variations over the equatorial Pacific Ocean

Clara Deser
CIRES, University of Colorado, Boulder

Abstract. Daily surface wind variations over the equatorial eastern Pacific Ocean during summer 1992 are documented, using hourly observations from the tropical atmosphere ocean moored buoy array. Diurnal and semidiurnal variations are apparent in the zonal wind component, with peak-to-peak amplitudes of a few tenths of a meter per second. The phase of the semidiurnal cycle in zonal wind is approximately uniform across the equatorial eastern Pacific Ocean, with westerly wind maxima at ~0300 and 1500 LT. The diurnal cycle dominates the daily march of meridional wind. The range of the diurnal meridional wind variations is ~0.6–0.8 ms^{-1} at most locations: more than twice as large as the daily zonal wind changes. The low-level flow is southward across the equator at night (relative to the daily mean), regardless of whether the mean winds are southerly or northerly. The diurnal meridional wind variations along the equator may be related to the diurnal cycle of deep convection in the Intertropical Convergence Zone (ITCZ) to the north. In particular, surface wind divergence along the equator (which is dominated by the meridional component) exhibits a pronounced diurnal cycle, with the strongest divergence in the early morning when deep convection in the ITCZ is at a maximum. The average daily range of the equatorial surface wind divergence is 1.5×10^{-6} s^{-1}, or ~30% of the daily mean. The semidiurnal zonal wind variations are dynamically consistent with the well-known semidiurnal cycle in surface pressure, which is thought to be a manifestation of the atmospheric thermal tide.

1. Introduction

Little is known about the magnitude and spatial pattern of daily surface wind variations over the open ocean in the tropics. (In this study, "daily" refers to all variations within a 24-hour period, and "diurnal" and "semidiurnal" refer to the first and second harmonics of the daily cycle, respectively.) Field programs such as the Global Atmospheric Research Program Atlantic Tropical Experiment (GATE) and the Barbados Oceanographic and Meteorological Experiment (BOMEX) gathered useful but limited information on daily wind changes in the tropical Atlantic [*Nitta and Esbensen*, 1974; *Gray and Jacobson*, 1977; *Pedder*, 1978; *McBride and Gray*, 1980; *Albright et al.*, 1981]. These studies emphasized the diurnal variation in the vertical profile of horizontal wind divergence and related the inferred upward motion to daily variations in deep convective activity. Diurnal wind variations at island stations in the western tropical Pacific were examined by *Wallace and Hartranft* [1969] and *Hastenrath* [1972]. These studies were concerned with the vertical structure of the diurnal wind changes in the troposphere and lower stratosphere and its relation to atmospheric tidal theory. A similar theme was pursued by *Williams and Avery* [1992], who documented the vertical structure of diurnal zonal wind variations at Christmas Island in the central equatorial Pacific. The only study to examine daily wind variability over the equatorial eastern Pacific is that by *Halpern* [1988]. He documented the diurnal surface wind amplitudes at four mooring sites along the equator east of 140°W.

The tropical atmosphere ocean (TAO) moored buoy array in the equatorial Pacific has been collecting hourly surface wind observations since ~1990 [*Hayes et al.*, 1991]. (Wind records at a few locations go back to ~1980 [*Halpern*, 1988].) The TAO array provides an unprecedented opportunity to study daily wind variability over a vast expanse of the equatorial ocean. The purpose of this study is to describe the large-scale spatial pattern of daily surface wind variations over the equatorial Pacific Ocean during summer 1992. This period contained the most complete data coverage at the time this investigation was undertaken. In addition to describing the diurnal and semidiurnal cycles of surface zonal and meridional wind, we investigate the daily variations of the large-scale surface wind divergence field over the equatorial eastern Pacific and relate those variations to the daily cycle of deep convection in the ITCZ.

Paper number 94JD02155.
0148-0227/94/94JD-02155$05.00

2. Data and Methods

Conceived by S. P. Hayes, the TAO array was designed to monitor upper ocean thermal conditions and surface atmospheric properties for improved prediction of the El Nino/Southern Oscillation cycle [*Hayes et al.*, 1991; *McPhaden*, 1993]. Beginning with two buoys in late 1983, the array in its fully implemented form in late 1994 will consist of 70 moorings distributed within 8° of the equator, spaced approximately every 15° of longitude across the Pacific basin [see *McPhaden*, 1993]. Winds are measured at ~3.8 m above the sea surface using cup and vane or propeller and vane assemblies (see *McPhaden and Hayes* [1990] and *Hayes et al.* [1991] for more details). The expected instrumental errors are typically ~0.1 ms^{-1}, with maximum calibration residuals less than 0.2 ms^{-1} for any particular instrument, based on predeployment and postdeployment calibration tests [*McPhaden and Hayes*, 1990; *Freitag et al.*, 1991]. Most of

Table 1a. Locations and Wind Sampling Characteristics of the 14 TAO Moorings Used in This Study

Buoy Location	Resolution	Averaging	No. of Days
5°N, 170°W	1 hour	centered	92
0°N, 170°W	1 hour	centered	92
5°N, 155°W	1 hour	centered	72
2°N, 155°W	1 hour	centered	92
0°N, 155°W	1 hour	centered	74
2°S, 155°W	1 hour	centered	75
5°S, 155°W	1 hour	centered	77
0°N, 140°W	1 hour	centered	92
2°S, 140°W	1 hour	centered	75
2°S, 125°W	1 hour	centered	92
5°S, 125°W	1 hour	centered	92
2°N, 110°W	1 hour	centered	92
0°N, 110°W	2 hours	beginning	91
2°S, 110°W	1 hour	centered	92

TAO, tropical atmosphere ocean. In column 3, "centered" means that the hourly or 2 hourly wind average is centered on the hour, and "beginning" means the hourly average is assigned to the beginning of the hour. Column 4 lists the number of days on which winds were measured during the 92-day period June 1–August 31, 1992.

the buoys provide hourly wind observations, but sampling within the hour is variable. At some buoys, winds are measured continuously, at others the "hourly" wind consists of a 6-min average centered on the hour, or of spot samples every 10 min (P. Freitag, personal communication, 1993). Depending on the buoy, the hourly values are assigned to either the beginning, the middle, or the end of the hour. The hourly wind data are recorded on cassette tape or solid state memory devices on board the buoys; the data tapes are retrieved every 6 months–1 year and processed at the TAO project office at the Pacific Marine Environmental Laboratory in Seattle, Washington.

This study uses data from the 92-day period June 1–August 31, 1992. Fourteen moorings reported hourly wind data on at least 60 days during this period; their locations and sampling characteristics are listed in Table 1a. The long-term (9 years) wind records at 0°, 110°W and 0°, 140°W are used to examine the seasonal dependence of the daily wind variations. The sampling characteristics for these buoys are given in Table 1b. All of the hourly or 2 hourly wind data used in this study were interpolated to the top of the hour.

3. Results

Daily Variations of Surface Wind

The mean surface wind field during summer 1992 from the TAO array is shown in Figure 1. Only those sites with at least 60 days of observations are included. Easterly winds

Table 1b. Wind Sampling Characteristics for the Buoys at 0°, 110°W and 0°, 140°W During 1983–1983

Buoy Location	Time Period	Resolution	Averaging
0°, 110°W	Nov. 1983 to April 1989	1 hour	beginning
	May 1989 to Oct. 1992	2 hours	beginning
0°, 140°W	April 1984 to April 1987	1 hour	beginning
	May 1987 to Oct. 1987	2 hours	beginning
	Nov. 1987 to Nov. 1988	1 hour	beginning
	Dec. 1988 to March 1990	2 hours	beginning
	April 1990 to April 1993	1 hour	centered

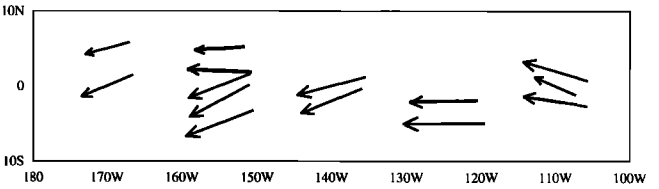

Figure 1. Mean surface wind field over the equatorial eastern Pacific during June–August 1992 from the tropical atmosphere ocean (TAO) array. Only those sites with at least 60 days of hourly observations are shown. The longest vector is 8 ms^{-1}.

prevail across the equatorial eastern Pacific, with magnitudes between 5 and 8 ms^{-1}. The winds exhibit a southerly component at 110°W and a northerly component west of 140°W. The mean winds over the equatorial eastern Pacific in summer 1992 were within 1–2 ms^{-1} of climatology [*Climate Analysis Center*, 1992].

Figure 2 shows the average daily march (in local time) of the zonal wind component during summer 1992 at all locations where data were reported on at least 60 days. The daily mean zonal winds have been removed and the hourly values smoothed with a three-point binomial filter. Positive (negative) values indicate westerly (easterly) winds relative to the daily mean. The 24-hour period has been repeated for clarity. The standard errors of the hourly wind averages are in the range 0.1–0.2 ms^{-1} for the set of buoy winds used here. Hence attention will be paid only to those daily wind changes that have peak-to-peak amplitudes ~0.3 ms^{-1} or greater. In Figure 2, diurnal and/or semidiurnal zonal wind variations are apparent at almost all of the sites, with peak-to-peak amplitudes of a few tenths of a meter per second. The semidiurnal fluctuations are particularly evident along 155° and 170°W where lower harmonics of the daily

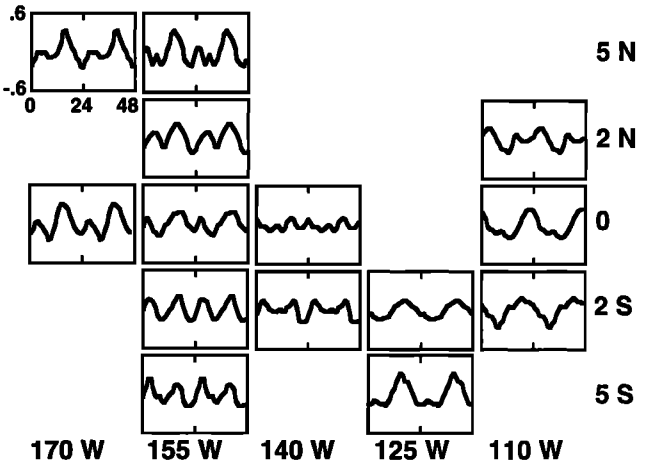

Figure 2. Average daily march of the zonal wind component in meters per second (ms^{-1}) during June–August 1992 from the TAO array. All boxes are drawn to the same scale, with local time on the abscissa (0–48 hrs) and wind speed on the ordinate (−0.6–0.6 ms^{-1}), as shown in the top left corner. The daily mean zonal winds have been removed from each site, and the hourly values smoothed with a three-point binomial filter. The 24-hour period is repeated for clarity. Positive (negative) values indicate westerly (easterly) winds relative to the daily mean.

cycle are suppressed. The phase and amplitude of the semidiurnal cycle is similar at all locations.

In contrast to the zonal wind the daily march of meridional wind exhibits a strong diurnal cycle with little semidiurnal variability (Figure 3). (In Figure 3, positive (negative) values indicate southerly (northerly) winds relative to the daily mean.) At most locations the range of daily meridional wind variations is ~1 ms^{-1}, almost twice as large as the daily range of the zonal wind variations. The low-level flow is southward across the equator at night (relative to the daily mean), regardless of whether the mean winds are southerly or northerly (see Figure 1). There appears to be a regular southward progression of the nighttime northerly wind maximum, particularly at 110° and 125°W (rate ~1 hour/deg of latitude).

To give an idea of the regularity of the daily wind cycles, Figure 4 shows the hourly meridional wind deviations from the daily means for each day during summer 1992 at 2°N, 155°W. Each column in Figure 4 shows the deviations from the daily means for a particular hour, with each dot representing a different day. The 24-hour period has been repeated for clarity. The daily cycle of meridional wind is visually apparent, but there is also a high proportion of scatter within each hour-column. It should be noted that the amplitude of the mean daily meridional wind cycle at 2°N, 155°W is among the largest of the set of buoy winds considered here (see Figure 3). The large proportion of scatter in Figure 4 underscores the need for lengthy, high-quality wind records with which to document daily cycles.

The wind records shown in Figures 2 and 3 were decomposed into diurnal and semidiurnal harmonics according to

$$X_k(t) = A_k \cos(\pi k/12t) + B_k \sin(\pi k/12t)$$

where X is the deviation of the zonal or meridional wind component from the daily mean, the index $k = 1$ ($k = 2$) refers to the diurnal (semidiurnal) harmonic, and t is time in hours. A_k and B_k were determined by the method of least squares [cf. *Draper and Smith*, 1966].

The amplitudes and phases of the diurnal and semidiurnal harmonics of zonal and meridional winds at each buoy are listed in Table 2. Figure 5a (Figure 5b) shows the amplitude

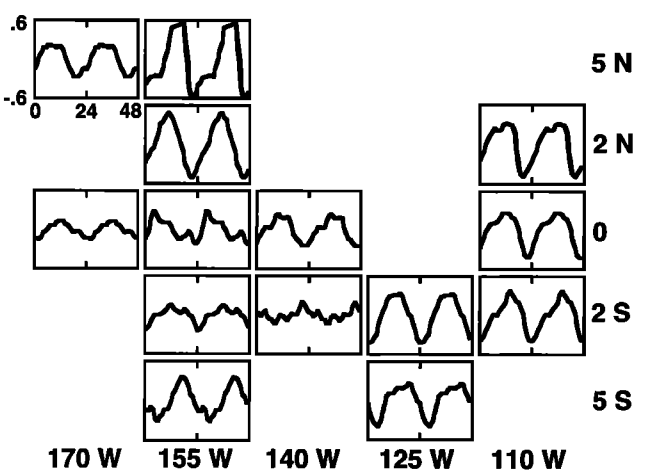

Figure 3. As in Figure 2 but for the meridional wind component (ms^{-1}). Positive (negative) values indicate southerly (northerly) winds relative to the daily mean.

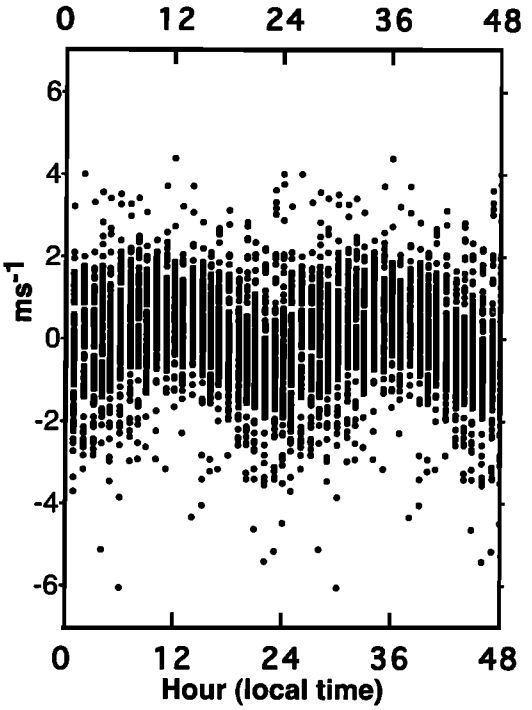

Figure 4. Scatter diagram of hourly meridional wind deviations from the daily means (ms^{-1}) for each day during summer 1992 at 2°N, 155°W. Each column shows the deviations from the daily means for a particular hour, with each dot representing a different day. The 24-hour period has been repeated for clarity.

and phase of the diurnal (semidiurnal) harmonic of the zonal wind component in vectorial format. The length of the arrow denotes the amplitude of the harmonic and the direction indicates the phase of the westerly wind maximum in local time. An arrow pointing due west indicates a local noon westerly maximum, with time increasing in the counterclockwise direction. The amplitudes of the diurnal and semidiurnal harmonics of zonal wind are comparable, with the majority of values around 0.15 ms^{-1} (see also Table 2). The phase of the semidiurnal harmonic of zonal wind (Figure 5b) is approximately uniform across the basin, with westerly maxima at ~0300 and 1500 LT (see also Table 2). The phase of the diurnal harmonic is less uniform than that of the semidiurnal harmonic, with the westerly wind maximum occurring in the evening at 110°W and in the afternoon elsewhere.

Figure 6 shows the harmonic analysis results for the meridional wind component. An arrow pointing due west indicates a local noon southerly wind maximum, with time increasing in the counterclockwise direction. The dominance of the diurnal harmonic (Figure 6a) over the semidiurnal harmonic (Figure 6b) is readily apparent. The amplitude of the diurnal meridional wind harmonic ranges from 0.09 ms^{-1} to 0.56 ms^{-1}, with values generally around 0.3–0.4 ms^{-1} (Table 2): more than twice as large as the mean amplitude of the diurnal harmonic of zonal wind (see Table 2). Southward phase propagation of the diurnal meridional wind harmonic is evident at 110°, 125°, and 155°W south of 1°N.

The amplitudes of the diurnal harmonics obtained in this study may be compared with those from previous studies.

Table 2. Amplitude (meters per second) and Phase (LT) of the Diurnal and Semidiurnal Harmonics of the Zonal and Meridional Wind Components at Each Buoy During June–August 1992

Zonal Wind	Diurnal Amplitude, ms^{-1}	Diurnal Phase, LT	Semidiurnal Amplitude, ms^{-1}	Semidiurnal Phase, LT
5°N, 170°W	0.14	1436	0.15	1606
0°N, 170°W	0.15	1612	0.17	1542
5°N, 155°W	0.15	1412	0.17	1400
2°N, 155°W	0.10	1306	0.15	1548
0°N, 155°W	0.12	1624	0.09	1430
2°S, 155°W	0.02	1442	0.17	1512
5°S, 155°W	0.03	0642	0.17	1512
0°N, 140°W	0.04	1754	0.03	1406
2°S, 140°W	0.05	0900	0.11	1530
2°S, 125°W	0.14	1618	0.02	1412
5°S, 125°W	0.21	1518	0.10	1518
2°N, 110°W	0.11	0030	0.10	1542
0°N, 110°W	0.19	2218	0.07	1530
2°S, 110°W	0.18	1906	0.03	1312
Meridional Wind	**Diurnal Amplitude, ms^{-1}**	**Diurnal Phase, LT**	**Semidiurnal Amplitude, ms^{-1}**	**Semidiurnal Phase, LT**
5°N, 170°W	0.25	0730	0.03	1300
0°N, 170°W	0.12	1124	0.02	0900
5°N, 155°W	0.56	1318	0.29	1436
2°N, 155°W	0.46	0932	0.06	1236
0°N, 155°W	0.17	0642	0.07	1142
2°S, 155°W	0.13	1230	0.05	1242
5°S, 155°W	0.29	1706	0.07	1024
0°N, 140°W	0.22	1000	0.05	1354
2°S, 140°W	0.09	2124	0.02	1554
2°S, 125°W	0.37	1236	0.05	1254
5°S, 125°W	0.28	1554	0.10	1536
2°N, 110°W	0.37	0930	0.14	1412
0°N, 110°W	0.30	1036	0.11	1530
2°S, 110°W	0.31	1312	0.10	1648

Nitta and Esbensen [1974] obtained diurnal harmonic amplitudes of 0.5 ms^{-1} for both wind components using 9 days of hourly wind data from BOMEX in the western Atlantic trades. *Pedder* [1978] reported diurnal harmonic amplitudes of 0.23 ms^{-1} for both wind components in his analysis of 21 days of 6 hourly wind data collected during GATE. *Halpern* [1988] found diurnal harmonic amplitudes ~0.18 ms^{-1} for the zonal wind component and ~0.34 ms^{-1} for the meridional wind component along the equator in the eastern Pacific using 1 year of hourly measurements. *Williams and Avery* [1992] obtained an amplitude of 0.15 ms^{-1} for the diurnal zonal wind harmonic at Christmas Island (2°N, 157°W) from 4 years of hourly profiler measurements. Hence the results reported here are compatible with those from previous studies.

Semidiurnal Cycle of Zonal Wind

The uniformity of phase of the semidiurnal cycle of zonal wind is striking (Figure 5b). It is well known that surface pressure in the tropics undergoes a strong semidiurnal variation [cf. *Haurwitz and Cowley*, 1973]. The local phase and amplitude of the semidiurnal pressure wave are approximately uniform within 20° of the equator, with pressure maximima at 0942 and 2142 LT and amplitude ~1 mbar [*Haurwitz and Cowley*, 1973; *Hamilton*, 1981]. This pressure

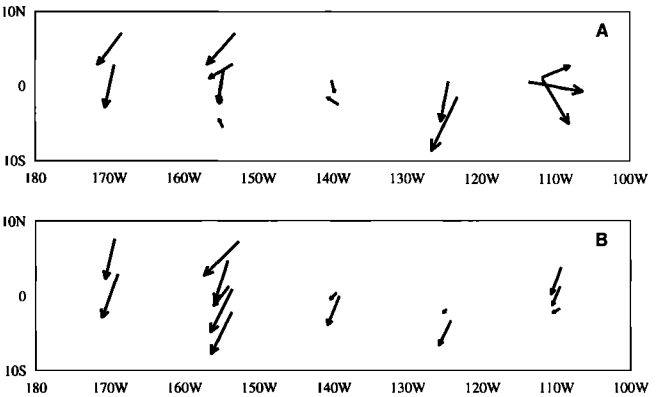

Figure 5. (a) Vector representation of the amplitude and phase of the diurnal harmonic of the zonal wind component during June–August 1992. The length of the arrow denotes the amplitude of the harmonic (ms^{-1}) and the direction indicates the phase in local time. An arrow pointing due west (south, east, north) indicates a westerly wind maximum at local noon (1800, 2400, 0600). The longest arrow is 0.25 ms^{-1}. (b) As in Figure 5a but for the semidiurnal harmonic of the zonal wind component. The arrow scale is the same for both panels.

wave is thought to be a manifestation of the thermal tide, due principally to the absorption of solar radiation by ozone in the stratosphere and water vapor in the troposphere [*Chapman and Lindzen*, 1970]. At the equator during June–July–August the semidiurnal surface pressure cycle may be expressed as [*Haurwitz and Cowley*, 1973]

$$P \text{ (mbar)} = 1.05 \sin (2t + 159°)$$

where t is local time in degrees. This pressure wave, shown graphically in Figure 7, migrates westward with the Sun, giving rise to zonal pressure gradients. The zonal wind (u) acceleration due to the semidiurnal pressure wave at the equator can be determined using a linear inviscid balance:

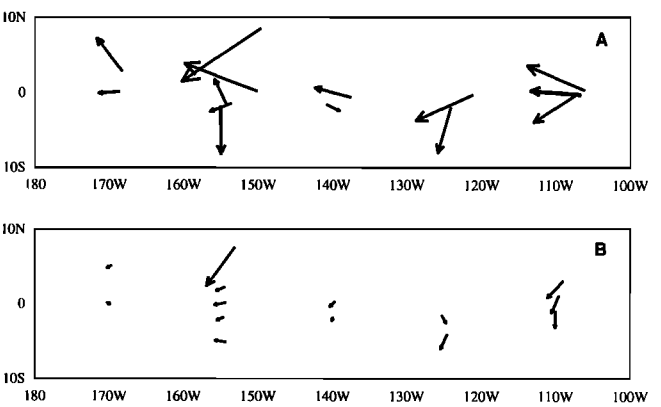

Figure 6. (a) As in Figure 5a but for the diurnal harmonic of the meridional wind component. An arrow pointing due west (south, east, north) indicates a southerly wind maximum at local noon (1800, 2400, 0600). The longest arrow is 0.6 ms^{-1}. (b) As in Figure 6a but for the semidiurnal harmonic of the meridional wind component. The arrow scale is the same for both panels.

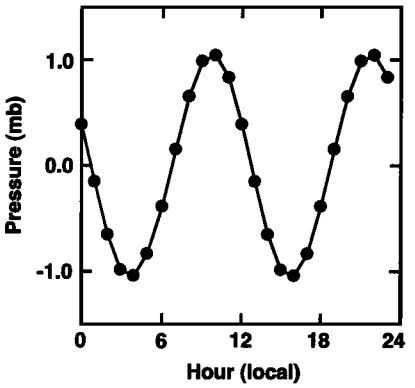

Figure 7. Semidiurnal cycle of sea level pressure (millibars) at the equator in local time [from *Haurwitz and Cowley*, 1973].

$$\delta u/\delta t = -1/\rho(\delta P/\delta x) \quad (1)$$

According to (1) the zonal wind will be a maximum (minimum) at 0400 and 1600 (1000 and 2200) LT when the pressure gradient vanishes. The predicted zonal wind is compared to the observed semidiurnal variation of zonal wind in the equatorial Pacific in Figure 8. To obtain a robust estimate of the observed semidiurnal cycle of zonal wind, the semidiurnal zonal wind harmonics at each buoy were averaged for each latitude band (5°N, 2°N, 0°, 2°S, 5°S) and then averaged together. Figure 8 shows there is good agreement between the observed and the predicted semidiurnal zonal winds at the equator. However, the amplitude of the predicted wind is larger than observed, and the phase is lagged by 1 hour.

The observed lack of a semidiurnal cycle in the meridional wind component (see Figure 3) is consistent with the lack of meridional variation in the semidiurnal pressure wave in the equatorial zone.

Daily Cycle of Surface Wind Divergence and Its Relation to Convection in the ITCZ

Studies by *Gray and Jacobsen* [1977] and *Hendon and Woodbury* [1993] have shown that rainfall over the open

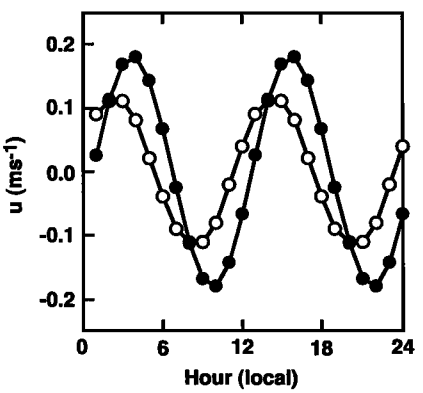

Figure 8. Observed (open circles) and predicted (solid circles) semidiurnal variation of the zonal wind component (ms^{-1}) at the equator in local time. The observed wind is an average for 5°N–5°S. The predicted wind is determined from the zonally averaged semidiurnal cycle of sea level pressure using a linear inviscid balance.

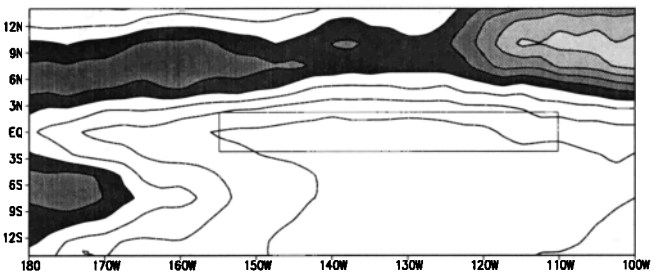

Figure 9. Distribution of outgoing longwave radiation (OLR) (watts per square meter) during June–August 1992. The contour interval is 10 W m^{-2} and values <240 W m^{-2} are shaded. The rectangle indicates the region for which surface wind divergence is calculated.

tropical ocean exhibits a strong diurnal cycle (amplitude ~1–2 mm d^{-1}), with the heaviest precipitation occurring in the early morning (0600–0900 LT). (*Hendon and Woodbury* [1993] inferred the diurnal variation of rainfall from an index of deep convective activity based on outgoing longwave radiation.) The Intertropical Convergence Zone (ITCZ) along ~8°N in the eastern Pacific exemplifies this behavior [*Hendon and Woodbury*, 1993]. Mechanisms responsible for the diurnal rainfall variations have been proposed by *Gray and Jacobsen* [1977] and *Randall et al.* [1991]. *Gray and Jacobsen* [1977] emphasize the role of day-night variations in tropospheric longwave cooling in clear versus cloudy regions, while *Randall et al.* [1991] advocate the role of day-night variations in cloud top heating and cooling. In simplest terms, deep convection in the ITCZ is associated with upward motion and low-level convergence locally and with large-scale compensating subsidence and low-level divergence to the north and south (i.e., a local Hadley circulation). This meridional circulation cell should exhibit a diurnal variation that is consistent with that in the convection. Specifically, the circulation should be strongest during early morning when the convection is most active and weakest during early evening.

Figure 9 shows the distribution of outgoing longwave radiation (OLR), a proxy for deep convection, over the tropical eastern Pacific during summer 1992. Convection in the ITCZ was active during summer 1992, as evidenced by the low OLR values (<240 W m^{-2}) along ~8°N. Wind data from buoys within the region (2°N–2°S, 155°W–110°W; see rectangle in Figure 9) were used to compute the mean daily variation of surface wind divergence during summer 1992. Note that the area used for the divergence calculation lies to the south of the ITCZ, in the region of compensating subsidence. Surface wind divergence south of the ITCZ exhibits a diurnal cycle, with divergence in the early morning and convergence in the early evening relative to the daily mean (Figure 10a). The phase of the diurnal cycle in surface wind divergence is thus consistent with that of deep convection in the ITCZ to the north. The mean daily range of the equatorial surface wind divergence is ~1.5×10^{-6} s^{-1}, or ~30% of the daily mean divergence (5.4×10^{-6} s^{-1}). The divergence is determined mainly by the meridional wind component (not shown).

The daily marches of meridional wind at 2°N and 2°S (the northern and southern boundaries of the region used to calculate the divergence) are shown in Figure 10b. The

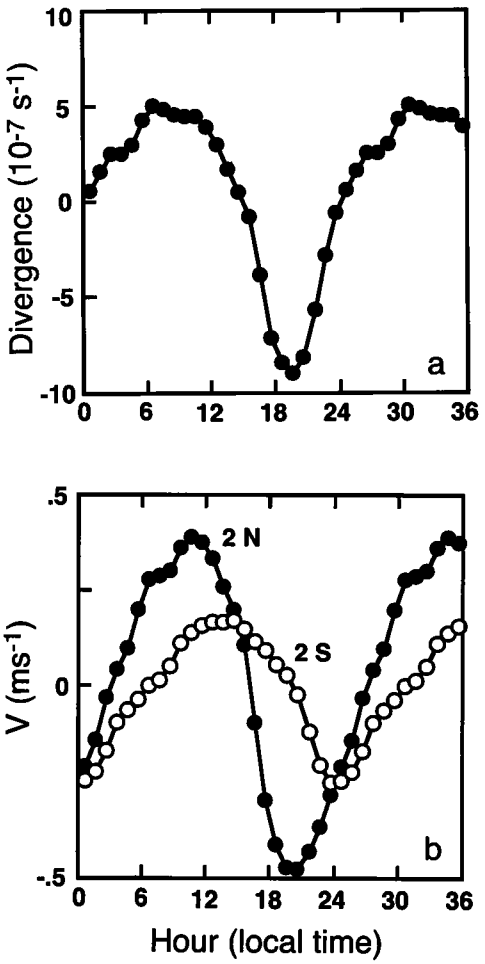

Figure 10. (a) Daily march of surface wind divergence (10^{-7} s^{-1}) during June–August 1992 for the region (2°N–2°S, 155°W–110°W). Times are local, with the first 12 hours repeated for clarity. The daily mean divergence has been removed. (b) Daily march of surface meridional wind (ms^{-1}) at 2°N and 2°S during June–August 1992. The winds have been averaged over the longitude band 155°–110°W and the daily means removed. Times are local, with the first 12 hours repeated for clarity.

winds have been averaged over the longitude band 155°–110°W. The diurnal cycle of meridional wind at 2°N leads that at 2°S by ~4 hours, and the amplitude is approximately twice as large.

The diurnal amplitude of the surface wind divergence is within the range of previous studies: *Nitta and Esbensen* [1974] obtained a diurnal amplitude of 2×10^{-6} s^{-1}; *Pedder* [1978] and *Wallace and Hartranft* [1969] reported amplitudes of 0.4×10^{-6} s^{-1} and 0.5×10^{-6} s^{-1}, respectively; and *Gray and Jacobsen* [1977] obtained an amplitude of 4×10^{-6} s^{-1} for days with deep convection. The phase of the surface wind divergence is also similar to that obtained by *Nitta and Esbensen* [1974], *Gray and Jacobsen* [1977], and *Albright et al.* [1981].

Figure 11 shows the mean wind vectors during summer 1992 at 0200, 0800, 1400 and 2000 LT. The wind vectors are deviations from the daily mean and represent 3-hour averages centered on the times given above. The 240 W m^{-2} OLR contour is also shown. The diurnal variation in convection is indicated schematically, with heavy shading for the strongest convection at 0800 LT, and no shading for the weakest convection at 0200 LT. At 0200 LT (Figure 11, top) the wind vectors are mostly northerly relative to the daily mean. By 0800 LT (Figure 11, top middle), when convection in the ITCZ is near its peak, the winds north of 2°S have become southerly (except at 5°N, 155°W). Equatorial divergence is clearly visible at this time. At 1400 LT (Figure 11, bottom middle), almost all of the wind vectors are southerly. By 2000 LT (Figure 11, bottom), when convection in the ITCZ is at a minimum, the winds north of 2°S have become northerly, resulting in convergence along the equator.

Seasonal Dependence of the Diurnal Wind Variations at 0°, 110°W and 0°, 140°W

Figure 12a shows the mean monthly amplitudes of the diurnal harmonic of meridional wind at 0°, 110°W and 0°, 140°W, based on the period 1984–1992. Both sites show a similar seasonal cycle, with the smallest diurnal amplitude (0.05 ms^{-1}) in spring (February–March–April) and the largest diurnal amplitude (0.35 ms^{-1}) in summer and autumn. The seasonal cycle of the diurnal meridional wind amplitude is compared to the seasonal cycle of OLR in the ITCZ

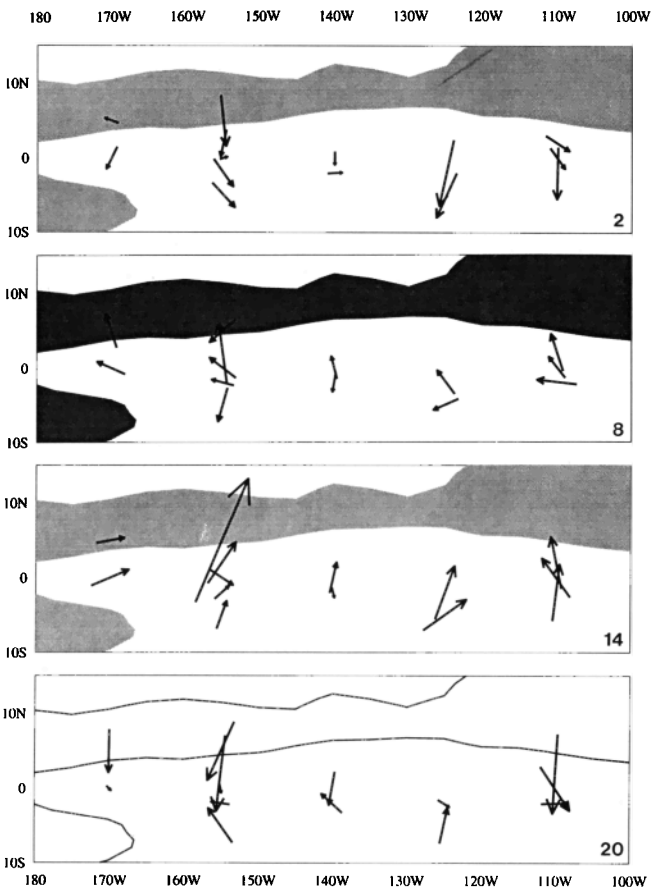

Figure 11. Mean wind vectors during June–August 1992 at 0200, 0800, 1400, and 2000 LT. The wind vectors are deviations from the daily mean and represent 3-hour averages centered on the times given above. The longest arrow is 0.8 ms^{-1}, and the arrow scale is the same for all panels. The 240 W m^{-2} OLR contour is also shown. The diurnal variation in convection is indicated schematically, with dark shading for the strongest convection at 0800 LT and no shading for the weakest convection at 2000 LT.

(Figure 12b). OLR was averaged over the area (9°–13°N, 150°–100°W] and the period 1984–1992. The meridional wind record shown in Figure 12b is the average of the diurnal harmonics at 0°, 110°W and 0°, 140°W. The seasonal cycles of both parameters are remarkably similar, with the largest diurnal wind amplitude occurring when convection is strongest and vice versa. While this comparison does not directly test the hypothesis that diurnal variations in deep convection are associated with diurnal variations in surface wind, it is suggestive, particularly in light of evidence presented by *Gray and Jacobsen* [1977], that the amplitude of the diurnal cycle in rainfall is proportional to the daily mean rainfall. A similar seasonal dependence of the daily surface wind variations at 0°, 150°E was reported by *Morrissey* [1990].

The mean monthly amplitudes of the diurnal and semidiurnal harmonics of zonal and meridional wind at 0°, 110°W and 0°, 140°W for 1984–1992 are listed in Table 3. None of the other harmonics exhibits as dramatic a seasonal variation as the diurnal harmonic of meridional wind. The semidiurnal harmonic of meridional wind is several times smaller than the diurnal harmonic in all months (except spring, when the amplitudes are negligible). The amplitudes of the diurnal and semidiurnal harmonics of zonal wind are comparable and modest (~0.05–0.15 ms^{-1}) in all months. Note that the amplitude of the diurnal zonal wind harmonic at 0°, 110°W during summer 1992 (0.19 ms^{-1}) was considerably larger than the long-term mean (0.11 ms^{-1}, Table 3).

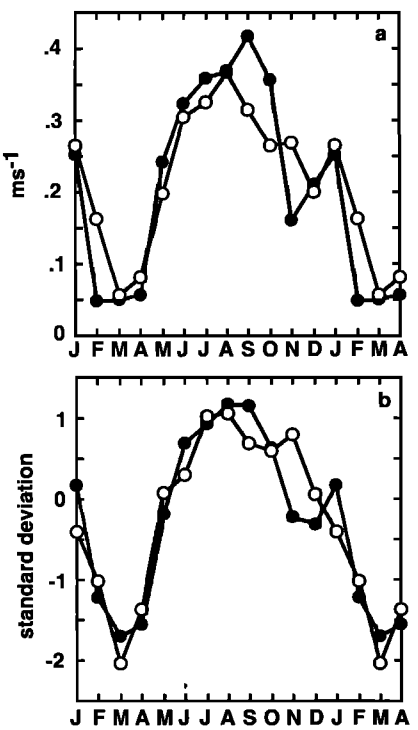

Figure 12. (a) Average seasonal cycle of the amplitude of the diurnal harmonic of meridional wind (ms^{-1}) at 0°, 110°W (solid circles) and 0°, 140°W (open circles), based on the period 1984–1992. The first four months have been repeated for clarity. (b) Average seasonal cycle of the amplitude of the diurnal harmonic of meridional wind at 0°, 110°W and 0°, 140°W averaged together (solid circles) and OLR in the ITCZ (9°–13°N, 150°–100°W) (open circles). Both records are standardized and the OLR data have been inverted so that positive (negative) values correspond to stronger (weaker) than average deep convection. Both the wind and the OLR records are based on the period 1984–1992.

Table 3. Mean Monthly Amplitudes (meters per second) of the Diurnal and Semidiurnal Harmonics of Zonal (U) and Meridional Wind (V) at 0°, 110°W and 0°, 140°W for 1984–1992

	U (0°, 110°W)		V (0°, 110°W)	
	Diurnal, ms^{-1}	Semidiurnal, ms^{-1}	Diurnal, ms^{-1}	Semidiurnal, ms^{-1}
January	0.08	0.07	0.25	0.16
February	0.07	0.10	0.05	0.07
March	0.16	0.08	0.05	0.02
April	0.23	0.09	0.06	0.02
May	0.14	0.02	0.24	0.08
June	0.08	0.03	0.32	0.10
July	0.12	0.07	0.36	0.07
August	0.13	0.05	0.37	0.09
September	0.10	0.03	0.42	0.08
October	0.07	0.05	0.36	0.12
November	0.12	0.06	0.16	0.11
December	0.11	0.07	0.21	0.13
	U (0°, 140°W)		V (0°, 140°W)	
	Diurnal, ms^{-1}	Semidiurnal, ms^{-1}	Diurnal, ms^{-1}	Semidiurnal, ms^{-1}
January	0.10	0.07	0.27	0.04
February	0.06	0.07	0.16	0.02
March	0.10	0.06	0.06	0.08
April	0.11	0.08	0.08	0.02
May	0.06	0.10	0.20	0.03
June	0.02	0.10	0.31	0.03
July	0.08	0.07	0.33	0.02
August	0.11	0.09	0.37	0.03
September	0.09	0.09	0.31	0.05
October	0.04	0.09	0.26	0.06
November	0.01	0.11	0.27	0.12
December	0.04	0.05	0.20	0.06

4. Summary

Daily variations of surface wind and wind divergence over the equatorial eastern Pacific during summer 1992 have been documented. The zonal wind component exhibits diurnal and semidiurnal variations of a few tenths of a meter per second. The phase of the semidiurnal cycle is approximately uniform over the domain, with westerly wind maxima at ~0300 and 1500 LT. The diurnal cycle dominates the daily march of the meridional wind component. The range of the diurnal meridional wind variations is ~0.6–0.8 ms^{-1} at most locations: more than twice as large as the daily zonal wind changes. The low-level flow is generally southward across the equator at night (relative to the daily mean), regardless of whether the mean wind is southerly or northerly. There is some evidence for a southward progression of the diurnal cycle of meridional wind.

The diurnal meridional wind variations along the equator may be related to the diurnal cycle of deep convection in the ITCZ to the north. In particular, surface wind divergence along the equator (which is dominated by the meridional component) exhibits a pronounced diurnal cycle, with the strongest divergence in the early morning when deep convection in the ITCZ is at a maximum. The average daily

range of the equatorial surface wind divergence is 1.5×10^{-6} s^{-1}, or ~30% of the daily mean.

The semidiurnal cycle in zonal wind is dynamically consistent with the observed zonally uniform semidiurnal cycle in surface pressure at the equator. The semidiurnal pressure wave is thought to be a manifestation of the atmospheric thermal tide [*Chapman and Lindzen*, 1970].

The TAO array is continuing to provide an unprecedented data set for the study of daily surface wind variations over the equatorial Pacific. The results presented here are based on a relatively short (92 days) period of record and sparse network of observations. A more comprehensive assessment of the daily wind variations is planned when the completed TAO array has been operational for several years.

Acknowledgments. I thank Michael J. McPhaden, director of the TOGA-TAO project, for his continuing interest in and support of this study. Linda Stratton, Linda Mangum, and Paul Freitag provided the wind data and crucial information on the hourly averaging procedures. I also thank William Gray for informative discussions on radiative forcing of the diurnal cycle and John M. Wallace and Harry Hendon for their valuable comments on an earlier draft of the manuscript. I gratefully acknowledge the hospitality of T. Vonder-Haar and CIRA, Colorado State University, where much of this work was completed. This study was supported by a grant from EPOCS.

References

Albright, M. D., D. R. Mock, E. E. Recker, and R. J. Reed, A diagnostic study of the diurnal rainfall variation in the GATE B-scale area, *J. Atmos. Sci.*, *38*, 1429–1445, 1981.

Chapman, S., and R. S. Lindzen, *Atmospheric Tides*, D. Reidel, Norwell, Mass., 1970.

Climate Analysis Center, *Climate Diagnostics Bulletin, August 1992*, 76 pp., U.S. Department of Commerce, National Oceanic and Atmospheric Administration, Washington, D. C., 1992.

Draper, N. R., and H. Smith, *Applied Regression Analysis*, 407 pp., John Wiley, New York, 1966.

Freitag, H. P., M. J. McPhaden, C. H. Coho, and A. J. Shepherd, Equatorial wind, current and temperature data: 108°W to 140°W, April 1983 to October 1987, *NOAA Data Rep. ERL PMEL-35*, 116 pp., Natl. Oceanic and Atmos. Admin., Washington, D. C., 1991.

Gray, W. M., and R. W. Jacobson Jr., Diurnal variation of deep cumulus convection, *Mon. Weather Rev.*, *105*, 1171–1188, 1977.

Halpern, D., Moored surface wind observations at four sites along the Pacific equator between 140° and 95°W, *J. Clim.*, *1*, 1251–1260, 1988.

Hamilton, K., Latent heat release as a possible forcing mechanism for atmospheric tides, *Mon. Weather Rev.*, *109*, 3–17, 1981.

Hastenrath, S. L., Daily wind, pressure and temperature variation up to 30 km over the tropical western Pacific, *Q. J. R. Meteorol. Soc.*, *98*, 49–59, 1972.

Haurwitz, B., and A. D. Cowley, The diurnal and semidiurnal barometric pressure oscillations: Global distribution and annual variation, *Pure Appl. Geophys.*, *102*, 193–222, 1973.

Hayes, S. P., L. J. Mangum, J. Picaut, A. Sumi, and K. Takeuchi, TOGA-TAO: A moored array for real-time measurements in the tropical Pacific Ocean, *Bull. Am. Meteorol. Soc.*, *72*, 339–347, 1991.

Hendon, H. H., and K. Woodberry, The diurnal cycle of tropical convection, *J. Geophys. Res.*, *98*, 16,623–16,637, 1993.

McBride, J. L., and W. M. Gray, Mass divergence in tropical weather systems, I, Diurnal variation, *Q. J. R. Meteorol. Soc.*, *106*, 501–516, 1980.

McPhaden, M. J., TOGA-TAO and the 1991–93 El Nino-Southern Oscillation event, *Oceanography*, *6*, 36–44, 1993.

McPhaden, M. J., and S. P. Hayes, Variability in the eastern equatorial Pacific during 1986–1988, *J. Geophys. Res.*, *95*, 13,195–13,208, 1990.

Morrissey, M. L., An evaluation of ship data in the equatorial western Pacific, *J. Clim.*, *3*, 99–112, 1990.

Nitta, T., and S. Esbensen, Diurnal variations in the western Atlantic Trades during BOMEX, *J. Meteorol. Soc. Jpn.*, *52*, 254–257, 1974.

Pedder, M. A., Diurnal and semidiurnal variations in the A/B Scale-averaged wind fields during phase III of GATE, *Mon. Weather Rev.*, *106*, 782–788, 1978.

Randall, D. A., Harshvardhan, and D. A. Dazlich, Diurnal variability of the hydrologic cycle in a general circulation model, *J. Atmos. Sci.*, *48*, 40–62, 1991.

Wallace, J. M., and F. R. Hartranft, Diurnal wind variations, surface to 30 km, *Mon. Weather Rev.*, *97*, 446–455, 1969.

Williams, C. R., and S. K. Avery, Comparison of observed diurnal and semidiurnal tropospheric winds at Christmas Island with tidal theory, *Geophys. Res. Lett.*, *19*, 1471–1474, 1992.

C. Deser, CIRES, University of Colorado, Campus Box 449, Boulder, CO 80309.

(Received March 15, 1994; revised August 15, 1994; accepted August 17, 1994.)